UNCLASSIFIED

SECURITY CLASSIFICATION OF THIS PAGE (When Data Entered)

ADA017088

REPORT DOCUMENTATION PAGE

READ INSTRUCTIONS BEFORE COMPLETING FORM

1. REPORT NUMBER	2. GOVT ACCESSION NO.
3. RECIPIENT'S CATALOG NUMBER	
4. TITLE (and Subtitle): Spectroscopic Studies of the Charge Transfer Reactions $He^+ + Hg \rightarrow He + (Hg^+)^*$ and $He_2^+ + N_2 \rightarrow 2He + (N_2^+)^*$ at Thermal Energy.	5. TYPE OF REPORT & PERIOD COVERED: Scientific Journal Article
	6. PERFORMING ORG. REPORT NUMBER: ~~APP-53~~, SRCC-216, APP-53
7. AUTHOR(s): Edward Graham, IV, Manfred A. Biondi and Rainer Johnsen	8. CONTRACT OR GRANT NUMBER(s): N00014-67-A-0402-0010
9. PERFORMING ORGANIZATION NAME AND ADDRESS: University of Pittsburgh, Pittsburgh, Pa. 15260	10. PROGRAM ELEMENT, PROJECT, TASK AREA & WORK UNIT NUMBERS: ARPA Order No. 2686
11. CONTROLLING OFFICE NAME AND ADDRESS: Advanced Research Projects Agency, 1400 Wilson Boulevard, Arlington, Virginia 22209	12. REPORT DATE: 16 October 1975
	13. NUMBER OF PAGES: 20
14. MONITORING AGENCY NAME & ADDRESS (if different from Controlling Office): Office of Naval Research, Arlington, Virginia 22217	15. SECURITY CLASS. (of this report): Unclassified
	15a. DECLASSIFICATION/DOWNGRADING SCHEDULE

16. DISTRIBUTION STATEMENT (of this Report)

Approved for public release; distribution unlimited.

17. DISTRIBUTION STATEMENT (of the abstract entered in Block 20, if different from Report)

DDC RELEASED NOV 11 1975

18. SUPPLEMENTARY NOTES

19. KEY WORDS (Continue on reverse side if necessary and identify by block number): non-resonant charge transfer, thermal energy charge transfer, excited state production, drift tube, helium-mercury laser, helium-nitrogen laser, Franck-Condon transition

20. ABSTRACT (Continue on reverse side if necessary and identify by block number)

The reactions $He^+ + Hg \rightarrow He + (Hg^+)^*$ and $He_2^+ + N_2 \rightarrow 2He + (N_2^+)^*$ have been studied at thermal energy in a drift tube-mass spectrometer apparatus fitted with a sapphire window for observing the light emitted from the electronically excited ions. For the first reaction, over the wavelength range 300-900 nm, the only emissions observed from the $(Hg^+)^*$ product ions are the 614.9 nm ($7p\ ^2P^o_{3/2} \rightarrow 7s\ ^2S_{1/2}$) and 794.4 nm ($7p\ ^2P^o_{1/2} \rightarrow 7s\ ^2S_{1/2}$) transitions, in approximately equal amounts. This equal branching in the case of reaction

DD FORM 1 JAN 73 1473 EDITION OF 1 NOV 65 IS OBSOLETE

UNCLASSIFIED

SECURITY CLASSIFICATION OF THIS PAGE (When Data Entered)

403 080

20. Abstract (cont'd.)

paths having substantially different energy defects, ΔE^{*} = 0.27 and 0.72 eV, respectively, is not explained by present theoretical models of the charge transfer process. For the second reaction, the emissions observed from the $(N_2^{+})^*$ product ions are from the first negative transition ($B^2\Sigma_u^+ \rightarrow X^2\Sigma_g^+$); the most intense lines observed and their corresponding vibrational levels are 391.4 nm (0,0), 427.8 nm (0,1), 470.9 nm (0,2), 522.8 nm (0,3) and 358.2 nm (1,0). The strongest of these lines is the 391.4 nm transition, with only a small intensity ($\lesssim$ 1% originating from the first vibrational level of the $B^2\Sigma_u^+$ state (358.2 nm), suggesting that undistorted Franck-Condon factors control the N_2^+ excitation-ionization during the charge transfer.

* delta E (Infinity)

APP-53

Spectroscopic Studies of the Charge Transfer Reactions $He^+ + Hg \rightarrow He + (Hg^+)^*$ and $He_2^+ + N_2 \rightarrow 2He + (N_2^+)^*$ at Thermal Energy

Edward Graham IV, Manfred A. Biondi and Rainer Johnsen

Physics Department, University of Pittsburgh

Pittsburgh, Pa. 15260

(Submitted to Physical Review)

Sponsored by
Advanced Research Projects Agency
ARPA Order No. 2686

This research was supported by the Advanced Research Projects Agency of the Department of Defense and was monitored by ONR under Contract No. N00014-67-A-0402-0010.

October 1975

Spectroscopic Studies of the Charge Transfer Reactions $He^+ + Hg \rightarrow He + (Hg^+)^*$ and $He_2^+ + N_2 \rightarrow 2He + (N_2^+)^*$ at Thermal Energy

Edward Graham IV, Manfred A. Biondi and Rainer Johnsen

Physics Department, University of Pittsburgh

Pittsburgh, Pa. 15260

Abstract

The reactions $He^+ + Hg \rightarrow He + (Hg^+)^*$ and $He_2^+ + N_2 \rightarrow 2He + (N_2^+)^*$ have been studied at thermal energy in a drift tube-mass spectrometer apparatus fitted with a sapphire window for observing the light emitted from the electronically excited ions. For the first reaction, over the wavelength range 300-900 nm, the only emissions observed from the $(Hg^+)^*$ product ions are the 614.9 nm ($7p\ ^2P_{3/2} \rightarrow 7s\ ^2S_{1/2}$) and 794.4 nm ($7p\ ^2P_{1/2} \rightarrow 7s\ ^2S_{1/2}$) transitions, in approximately equal amounts. This equal branching in the case of reaction paths having substantially different energy defects, $\Delta\varepsilon(\infty)$ = 0.27 and 0.72 eV, respectively, is not explained by present theoretical models of the charge transfer process. For the second reaction, the emissions observed from the $(N_2^+)^*$ product ions are from the first negative transition ($B^2\Sigma_u^+ \rightarrow X^2\Sigma_g^+$); the most intense lines observed and their corresponding vibrational levels are 391.4 nm (0,0), 427.8 nm (0,1), 470.9 nm (0,2), 522.8 nm (0,3) and 358.2 nm (1,0). The strongest of these lines is the 391.4 nm transition, with only a small intensity ($\lesssim$ 1%) originating from the first vibrational level of the $B^2\Sigma_u^+$ state (358.2 nm), suggesting that undistorted Franck-Condon factors control the N_2 excitation-ionization during the charge transfer.

I. Introduction

Under favorable conditions non-resonant charge transfer (NRCT) can be a fast process and further can leave the ion in an electronically excited state. Two reactions which exhibit these properties are

$$He^+ + Hg \rightarrow He + (Hg^+)^* \qquad (1)$$

and

$$He_2^+ + N_2 \rightarrow 2He + (N_2^+)^* \quad , \qquad (2)$$

where the asterisk superscript indicates an electronically excited state. The total rate coefficients for both reactions have been determined previously; at thermal (300K) energies, $k_1 = (1.6 \pm 0.3) \times 10^{-9}$ cm^3/sec[1] and $k_2 = (1.3 \pm 0.4) \times 10^{-9}$ cm^3/sec[2]. As will be discussed later, in both reactions it appears that certain slightly exothermic channels are favored which involve formation of the product ions in particular excited states.

The present work has been conducted both to obtain information concerning which of these excited states are produced and to demonstrate the feasibility of observing photon emission from ions produced by reactions in a drift mobility tube at low energies (300K). By combining mass analysis of the ions and spectroscopic analysis it has been possible to identify positively the electronically excited states produced in particular NRCT reactions.

II. Apparatus

The present studies were conducted using a drift tube - mass spectrometer apparatus of ultra-high vacuum construction. Since the basic apparatus (Fig. 1) has been described in detail elsewhere[3], only a brief

description will be given here. The modifications to permit optical emission studies are described in some detail.

Ions are produced in a differentially pumped source by electron bombardment and are periodically gated through a small hole ($\sim$ 0.020" ϕ) into the drift region which is filled with gas to a pressure typically between 0.05 and 2 Torr. A uniform electric field E is maintained in the drift region by the cylindrical guard rings. Once in the drift region the ions quickly reach a steady drift condition, moving axially in the direction of the electric field. In addition to this general axial drift the ions diffuse radially and axially due to collisions with the gas molecules and also may undergo ion-molecule reactions. At the end of the drift region there is another small hole (0.020" ϕ) leading to a differentially pumped region containing an rf quadrupole mass filter. Those ions effusing through this hole are accelerated into the mass filter, selected according to their charge/mass ratio, and detected by a channel electron multiplier operating in a pulse counting mode. The pulses from the multiplier are amplified, discriminated, and sorted according to their time of arrival in a multi-channel analyzer. (The time t = 0 is defined as the time when the ions are admitted to the drift region.)

For the present experiment a hole approximately 2 cm square was cut in a guard ring to allow optical viewing of the interior of the drift region (see Fig. 1). This opening is crossed with small wires to insure that the electric field in the drift region remains uniform. A sapphire window forms the vacuum seal and transmits radiation over the wavelength range $\sim 200 \leq \lambda \leq \sim 5000$ nm. A unit magnification optical system consisting of an achromat lens and a first surface mirror images the radiation from the drift tube onto the entrance slit of the monochromator. The diameter of the lens and the imaging distance yield an effective f-value

f/5.0, compatible with the f/5.3 value of the McPherson Model 218 scanning monochromator. The grating employed has 1200 grooves/mm and is blazed at 5000Å.

The exit slit of the monochromator is imaged by another achromat lens onto an EMI type 9658A or an RCA type CA31034A photomultiplier tube. The dark counting rate of the photomultiplier tube is reduced by cooling with dry ice and in the case of the EMI 9658A by use of a magnetic lens to reduce the effective cathode area. With this procedure, the dark counting rate is $\leq$ 5 counts/sec. The photomultiplier is operated in a pulse counting mode, and these pulses are sorted according to their time of arrival, exactly as the ions detected by the mass filter are sorted.

It was found that some light was created in the ion source and reflected from metal surfaces in the drift region into the optical viewing cone. This background light was reduced in two ways. The surfaces of the guard rings that could be viewed by the monochromator, i.e. the area opposite the hole cut in the guard ring and the area around the hole, were coated with aquadag to produce a flat gray-black surface. Reflections from outside the guard rings were further reduced by inserting a cylindrical baffle around the optical path as shown in Fig. 1. The inside of the optical baffle was coated with carbon from an acetylene flame, producing an excellent flat-black matte finish.

The wavelength range of the present apparatus is $300 \leq \lambda \leq 900$ nm. This range can be altered or extended without having to open the vacuum system simply by changing grating, photomultiplier and lenses.

III. Results

A. $He^+ + Hg$

The He^+ ions are created by electron bombardment of helium gas introduced through the inlet capillary into the differentially pumped ion source region. Some of these ions enter the drift region, which typically contains 0.3 Torr of He and 0.2 mTorr of Hg, and undergo non-resonant charge transfer with Hg atoms. Since the production of $(Hg^+)^*$ ions by reaction (1) is detected through the emission of photons, it is necessary that the ions emit within the volume "seen" by the monochromator and that the emission direction lie within the solid angle Ω subtended by the optics. For emission from an ion on-axis directly beneath the optical window the fractional solid angle $\Omega/4\pi$ is $\sim 10^{-3}$. Considering instrumental transmission and reflection factors and photomultiplier sensitivity, approximately 1 in 10^4 of the photons emitted from the observable volume is counted.

The only emissions detected from the radiative decay of the $(Hg^+)^*$ product ions are the 614.9 nm ($7p\ ^2P_{3/2} \rightarrow 7s\ ^2S_{1/2}$) and the 794.4 nm ($7p\ ^2P_{1/2} \rightarrow 7s\ ^2S_{1/2}$) transitions. As shown in Table I, the $^2P_{3/2}$ and $^2P_{1/2}$ states have energy defects $\Delta\varepsilon(\infty)$ of 0.27 and 0.72 eV, respectively, for reaction (1). No radiation is detected from other nearby states with allowed transitions to the $7s\ ^2S_{1/2}$ levels, even though their energy defects are intermediate between those of the two observed levels. Possible reasons for this behavior are discussed in the next section. The intensity ratio I(794.4)/I(614.9) has been calculated from the observed photon counting rates and the measured spectral sensitivity of the apparatus (determined with the aid of a low brightness source). The ratio is found to be 0.7, with an estimated uncertainty of $\pm$ 20%.

B. $He_2^+ + N_2$

The drift region is filled typically with 2 Torr of He and 1 mTorr of N_2. The He^+ ions created by electron bombardment of helium in the source region enter the drift region where they react with the He and N_2 to produce He_2^+, N^+, and N_2^+ through the reactions:

$$He^+ + 2He \rightarrow He_2^+ + He \qquad (3)$$

and

$$He^+ + N_2 \begin{cases} \rightarrow He + N^+ + N \\ \rightarrow He + N_2^+ \end{cases} . \qquad (4)$$

The He_2^+ ions formed by reaction (3) may then react to produce N_2^+ ions in an excited state by the charge transfer reaction (2).

The relatively high pressure of helium (2 Torr) acts to increase the rate of production of He_2^+ from He^+. (It also inhibits radial diffusion of the He_2^+ ions, thereby ensuring that the product ions are produced sufficiently close to the axis that the emitted photons are observable.) Two distinct types of emission are observed, the He I spectrum and the first negative transition of N_2^+ ($B^2\Sigma_u^+ \rightarrow X^2\Sigma_g^+$). The He I spectrum has been determined to be ion source produced and thus is not of interest in the present research. The N_2^+ spectrum is shown to originate from $(N_2^+)^*$ ions produced via reaction (2).

Figure 2 shows the arrival time spectra of He^+ and He_2^+ ions as detected by the ion sampling system and the arrival time spectrum of the 391.4 nm emission from the $(N_2^+)^*$ decay as detected by the optical system. That the $(N_2^+)^*$ is produced from He_2^+ and not He^+ is determined as follows: (a) As the He pressure in the drift region is increased the number of He^+ ions decreases as a result of reaction (3), with a consequent increase in the number of He_2^+ ions. A corresponding increase in the 391.4 nm emission

is observed. (b) For a short-lived transition such as the $B^2\Sigma_u^+ \rightarrow X\ ^2\Sigma_g^+$, the peak intensity should occur when the parent ions which produce the $(N_2^+)^*$ are directly beneath the window. Since the window is located approximately midway between the entrance and exit orifice of the drift tube, the time of the peak 391.4 nm intensity should be approximately one half the parent ion's transit time to the exit orifice. From the arrival time spectra of Fig. 2 it will be seen that He_2^+ rather than He^+ is the parent ion.

The observed first negative band emissions and their corresponding vibrational levels are 391.4 nm (0,0), 427.8 nm (0,1), 470.9 nm (0,2), 522.8 nm (0,3), and 358.2 nm (1,0). The strongest of these lines is the 391.4 nm transition, with the higher vibrational transitions becoming progressively less intense. The observed ratio between the 391.4 nm (0,0) and the 427.8 nm (0,1) signals is 1.9, rather smaller than the emission intensity ratio 3.1 observed by Shemansky and Broadfoot[4]. Only a small signal ($\leq$ 1%) originates from the first vibrational level of the $B^2\Sigma_u^+$ state (358.2 nm).

IV. Discussion

The drift tube - mass spectrometer - optical spectrometer apparatus offers advantages over discharge or afterglow techniques for studies of NRCT reactions. Not only can one identify the product ions and any (radiating) excited states in which they are formed, but one can also identify unequivocally the parent ions responsible for the reaction. Also, production of excited ions by reactions other than charge transfer (e.g. metastable atom reactions) are ruled out in the drift tube studies, while in discharge and afterglow studies considerable care must be taken to distinguish among the various sources of the excited ions.

$He^+ + Hg$

The most interesting result of the present spectroscopic study of this NRCT reaction at thermal energies is that the branching ratio for production of the $(Hg^+)^*$ ions in the $^3P_{1/2}$ and $^3P_{3/2}$ states is approximately unity, even though the energy defects for the two reaction channels are quite different, $\Delta\epsilon(\infty)$ = 0.72 and 0.27 eV, respectively. The failure to detect production of any of the $(5d)^9 6s6p$ states having intermediate energy defects (see Table I) suggests that these states have a small chance for formation by the NRCT process. This possibility is at least consistent with a curve-crossing model of the NRCT process[5], since it is to be expected that the $(He\text{-}Hg)^+$ molecular states formed from $(5d)^9 6s6p$ states of Hg^+ are less repulsive than those from the $(5d)^{10} 7p$ states owing to the smaller extent of the 6p orbital compared to the 7p. Thus, as illustrated schematically in Fig. 3, curve-crossings will occur at longer range for the ^2P states, leading to favored branching into these final states.

The main problem is to account for the essentially <u>equal</u> population of $^2P_{1/2}$ and $^2P_{3/2}$ Hg^+ final states. For the analagous case of $He^+ + Zn$, in a modification of the pseudo-crossing theory of Turner-Smith et al.[5], Melius[6] has presented arguments to account for the observed branching ratio[5] of 0.13 into the $^2P_{1/2}$ and $^2P_{3/2}$ fine structure levels of $(Zn^+)^*$. He argues that the only important outer crossing is the $^2\Sigma_{1/2} - {}^2\Sigma_{1/2}$ pseudo-crossing (equivalent to position 1 in Fig. 3) which correlates adiabatically with the $^2P_{3/2}$ state of $(Zn^+)^*$, since the $^2\Pi_{1/2}$ states correlating with the $^2P_{3/2}$ and $^2P_{1/2}$ states are only weakly repulsive. Thus, under near-adiabatic conditions, production of the $^2P_{3/2}$ state is highly favored and the nearby $^2P_{1/2}$ state (fine structure splitting = 0.009 eV) can only be produced by coupling between the $^2\Sigma_{1/2}$ (p_σ) and $^2\Pi_{1/2}$ (p_π) states as the collision partners separate.

This argument fails in the present case of $He^+ + Hg$, since the fine structure splitting between the $^2P_{1/2}$ and $^2P_{3/2}$ levels is much greater, 0.45 eV, leading to decreased coupling, yet the branching ratio into $^2P_{1/2}$ is larger, 0.7. The direct production of the $^2P_{1/2}$ state by rotational coupling at the crossing of the $^2\Pi$ final state curve with the $^2\Sigma$ initial state curve (position 2 in Fig. 3) has not been discussed in the curve-crossing theories[5,6] and its effect is difficult to assess. Therefore, we conclude that the observed large branching ratio into the $^2P_{1/2}$ state can not be explained in terms of present theoretical descriptions of the NRCT process.

The fact that the $He^+ + Hg$ charge transfer process, reaction (1), provides the inversion mechanism for lasing at 614.9 nm in helium-mercury discharges was evidently first recognized by Dyson[7], who obtained an estimate of the charge transfer frequency from measured 614.9 nm intensity decay rates following a current pulse in a helium-mercury mixture. He expressed his results as an average reaction cross section, $\langle \sigma_1 \rangle = 1.3 \times 10^{-14}$ cm^2, which yields a rate coefficient in excellent agreement with our previous drift tube results[1], $k_1 = (1.6 \pm 0.3) \times 10^{-9}$ cm^3/sec at 295 K. Very recently, Dyson's results have been confirmed by Kano et al.[8] in similar intensity decay studies (of both 614.9 and 794.4 nm radiation) in helium-mercury afterglows. They find a branching ratio for $^2P_{1/2}:^2P_{3/2}$ state formation of ~ 1.9, a value even larger than our value of 0.7. (Our result, obtained from measurements in which NRCT should be the only source of the excited ions, should be accurate.)

This very large charge transfer rate coefficient is close to an upper limit value calculated on the assumption that <u>all</u> collisions that involve impact parameters within the Langevin spiralling limit result

in NRCT, i.e.

$$k_{max} = k_{Langevin} = 2\pi[\alpha e^2/\mu]^{\frac{1}{2}} = 2.6 \times 10^{-9} \text{ cm}^3/\text{sec} \quad , \qquad (5)$$

where α is the dipole polarizability of Hg (5.02Å^3) and μ is the reduced mass of the He^+ - Hg system. In theories involving transitions between initial and final states at crossings or pseudo-crossings of the potential curves, the net charge transfer probability $\mathcal{P} = 2P(1-P)$ for a single curve crossing reaches a maximum value of 1/2 when P, the transition probability at a single pass (incoming or outgoing), is 1/2. However, with multiple exit channels (multiple crossings) such as illustrated in Fig. 2 values of $\mathcal{P} > 1/2$ are possible. The He^+ + Hg reaction may well be such a case.

$He_2^+ + N_2$

In the case of NRCT processes involving molecular species, constraints in addition to the requirement of a small energy defect must be considered. In previous studies[9] of the reaction

$$He^+ + H_2 \rightarrow He + H^+ + H \quad , \qquad (6)$$

in the vicinity of energy-resonance the lack of an allowed vertical Franck-Condon transition between the H_2 ground state and the predissociating H_2^+ state appears to account for the small reaction rate ($\sim 10^{-13}$ cm^3/sec) at thermal energies. Thus, Franck-Condon overlap factors evidently play a role in determining the reaction rate.

In the present studies of the $He_2^+ + N_2$ charge transfer, reaction (2), the process is fast, yet the vibrational state of the $N_2^+(B^2\Sigma_u^+)$ excited ions is not that which would make the reaction most nearly energy resonant. (Refer to the potential curves of Fig. 4 which are taken from the literature[10].

The light vertical lines indicate the classical turning points for the v = 0 states of the N_2 and He_2^+.) If energy resonance were the determining factor, the $v \sim 4$ level of the $B^2 \Sigma_u$ state would be populated (assuming small distortion of the He_2^+ and N_2 potential curves during the collision). However, the spectroscopic observations indicate that the v = 0 and to a much lesser extent the v = 1 states of $B^2 \Sigma_u^+$ are populated by the reaction, which is just the behavior expected if Franck-Condon factors appropriate to the undistorted N_2 potential curves apply. Here again we are led to the conclusion that essentially undistorted Franck-Condon overlap factors come into play in determining the final states in NRCT processes involving molecules.

The production of $(N_2^+)^*$ excited ions by NRCT from He_2^+ has been shown by Collins et al.[11] to provide the population inverting mechanism in a new e-beam pumped helium-nitrogen laser emitting at 427.8 nm. In order to assess the potential of this process for laser applications, one needs to know the relative probabilities for production of the various states of N_2^+(e.g. $B^2 \Sigma_u^+$, $A\ ^2\Pi_u$, $X\ ^2\Sigma_g^+$). Unfortunately, at present none of the present methods of measuring NRCT provide this information. In the present experiment it is possible to determine the absolute yield of (radiating) excited ions by absolute intensity determinations, but it is not possible to determine absolute numbers of positive ions with the quadrupole mass spectrometer. Since a charge collecting electrode at the exit of the drift tube could provide the required information, in future studies it may be possible to obtain the ratio of excited product ion yield to total product ion yield.

Acknowledgement

The authors are indebted to J. N. Bardsley for helpful discussions of the various steps involved in the non-resonant charge transfer process. This research was supported, in part, by the Advanced Research Projects Agency of the Department of Defense and was monitored by ONR under Contract No. N00014-67-A-0402-0010.

References

1. R. Johnsen, M. T. Leu and M. A. Biondi, Phys. Rev. A8, 1808 (1973).
2. F. C. Fehsenfeld, A. L. Schmeltekopf, P. D. Goldan, H. I. Schiff, and E. E. Ferguson, J. Chem. Phys. 44, 4087 (1966).
3. R. Johnsen and M. A. Biondi, J. Chem. Phys. 59, 3504 (1973).
4. D. E. Shemansky and A. L. Broadfoot, J. Quan. Spec. and Rad. Trans., 11, 1385 (1971).
5. A. R. Turner-Smith, J. M. Green, and C. E. Webb, J. Phys. B: Atom. Molec. Phys. 6, 114 (1973).
6. C. F. Melius, J. Phys. B: Atom. Molec. Phys. 7, 1692 (1974).
7. D. J. Dyson, Nature, 207, 361 (1965).
8. H. Kano, T. Shay and G. J. Collins, Appl. Phys. Lett., to be published, (Dec. 1975).
9. R. Johnsen and M. A. Biondi, J. Chem. Phys. 61, 2112 (1974).
10. W. B. Maier II, J. Chem. Phys. 62, 4615 (1975).
11. C. B. Collins, A. J. Cunningham and M. Stockton, Appl. Phys. Lett. 25, 344 (1974).

Table I. Properties of some $(Hg^+)^*$ excited states involved in the $He^+ + Hg \rightarrow He + (Hg^+)^*$ charge transfer reaction.

Configuration	Designation	J	$\Delta\epsilon(\infty)$, eV	Transition to $(5d)^{10}7s[^2S_{1/2}]$, nm	Relative Intensity
$(5\ d)^{10}[^1S]7p$	$7p\ ^2P^o$	3/2	0.27	614.9	1
$(5d)^9\ 6s\ 6p$	-	7/2	0.37	(646.9)[b]	$< 10^{-2}$
$(5d)^9\ 6s\ 6p$	-	7/2	0.41	(660.9)	$< 10^{-2}$
$(5d)^9\ 6s\ 6p$	-	3/2	0.44	671.6	$< 10^{-2}$
$(5d)^9\ 6s\ 6p$	$^2P^o$	3/2	0.61	742.1	$< 10^{-2}$
?	-	7/2	0.64	(754.1)	$< 10^{-2}$
$(5d)^{10}[^1S]7p$	$7p\ ^2P^o$	1/2	0.72	794.4	0.7

(a) C. E. Moore, Atomic Energy Levels, Vol. III, National Bureau of Standards Circular 467, (Supt. Documents, U. S. Gov't. Printing Office, Washington, D. C., 1958).

(b) Wavelengths in parentheses indicate transitions "forbidden" by the $\Delta J \neq 2$ selection rule, although such transitions are observed in the neutral Hg spectrum.

Figure Captions

Fig. 1 Simplified diagram of the drift tube-mass spectrometer-optical spectrometer apparatus.

Fig. 2 Arrival time spectra of the He^+ and He_2^+ ions at the exit orifice of the drift tube and the 391.4 nm $(N_2^+)^*$ radiation intensity observed at the midway viewing port in the drift tube under essentially thermal (300 K) energy conditions, $E/p = 1.8$ V-cm^{-1}-Torr^{-1}. A trace of N_2 is added to the He to produce the $(N_2^+)^*$ spectrum.

Fig. 3 Highly schematic potential curves for the $(He - Hg)^+$ system, indicating the long range attractive $-C/R^4$ polarization potential for He^+-Hg, the repulsive potential curves associated with the $(5d)^{10}7p$ states of Hg^+ and the weaker repulsive curves associated with the $(5d)^9$ 6s 6p states of Hg^+.

Fig. 4 Potential energy curves for the N_2 and He_2^+ systems illustrating the energetics of the $He_2^+ + N_2$ charge transfer reaction. The light vertical lines indicate the classical Franck-Condon regions for N_2 and He_2^+ in their v = o vibration states.

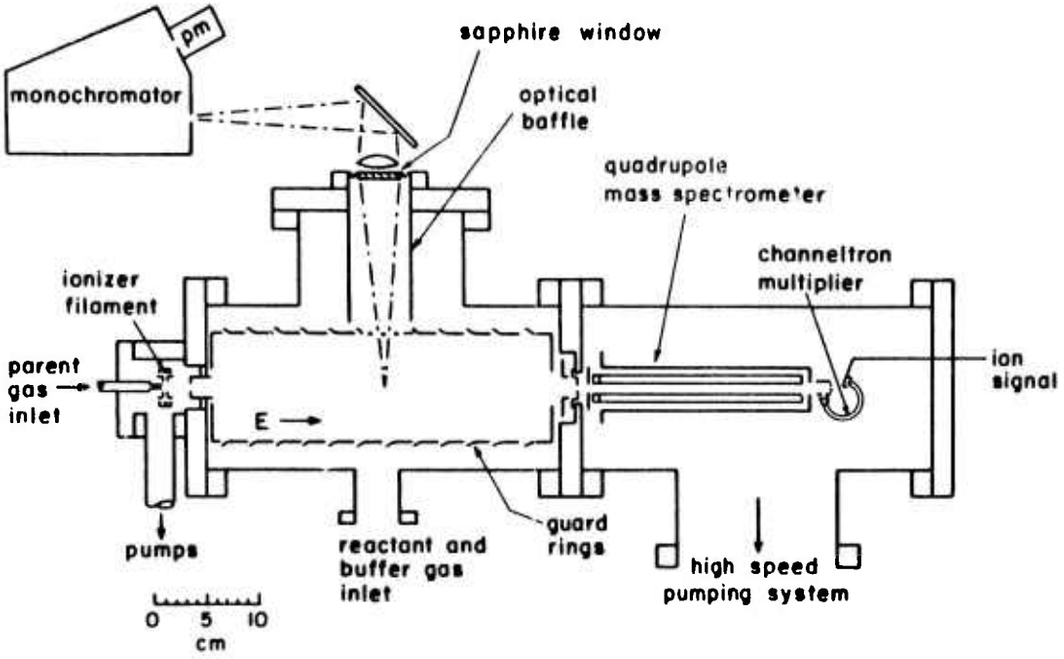
pm
monochromator
sapphire window
optical baffle
quadrupole mass spectrometer
channeltron multiplier
ionizer filament
parent gas inlet
E
ion signal
pumps
reactant and buffer gas inlet
guard rings
high speed pumping system
0 5 10
cm

Figure 1

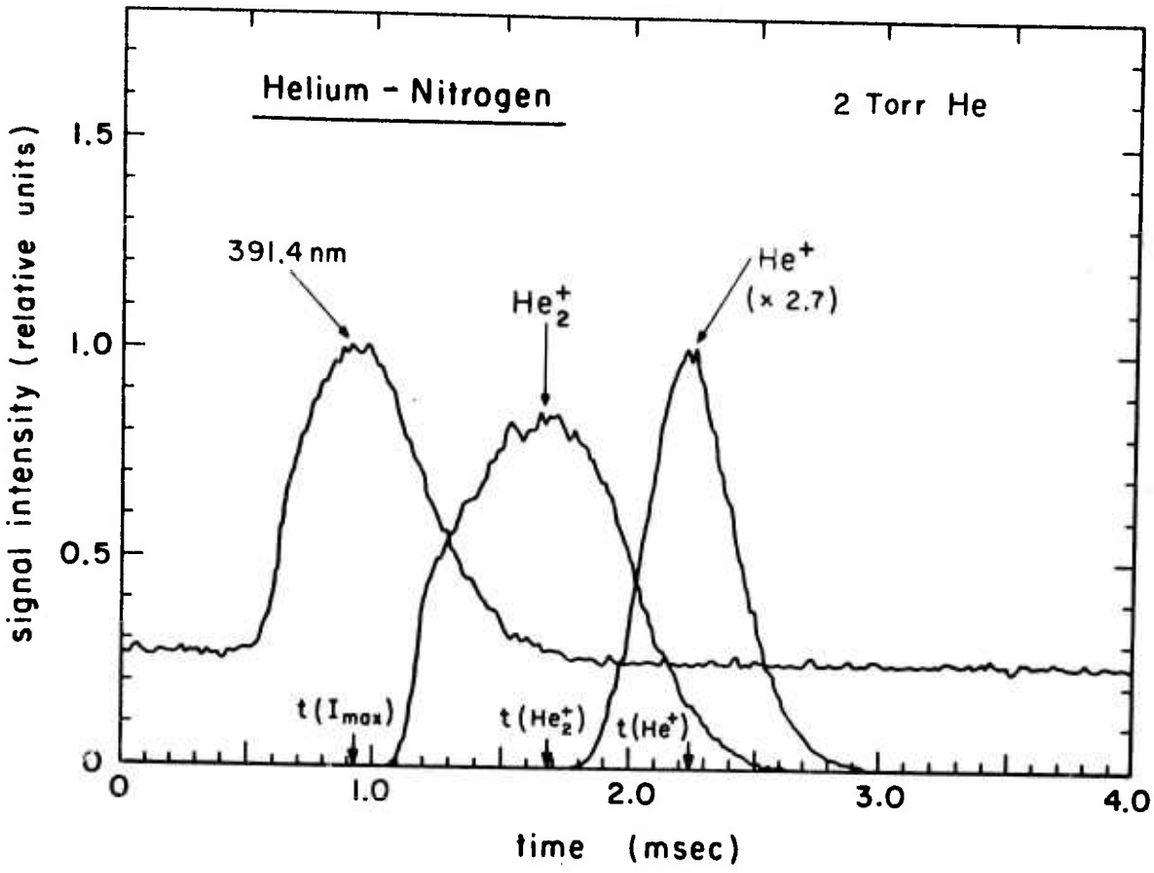
Helium - Nitrogen
2 Torr He
391.4 nm
He_2^+
He^+
(× 2.7)
signal intensity (relative units)
1.5
1.0
0.5
0
$t(I_{max})$
$t(He_2^+)$
$t(He^+)$
0
1.0
2.0
3.0
4.0
time (msec)

Figure 2

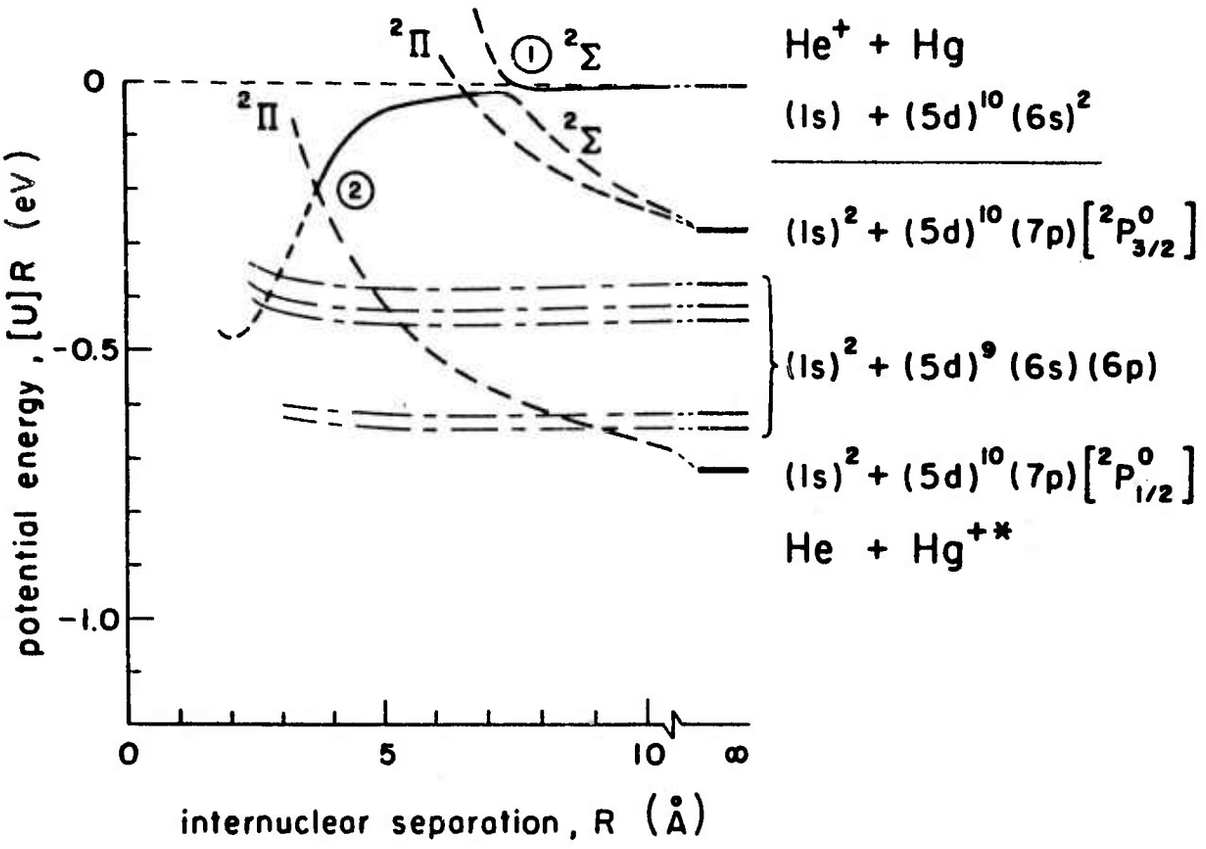
$^2\Pi$
① $^2\Sigma$
$^2\Pi$
$^2\Sigma$
②
0
-0.5
-1.0
potential energy , [U]R (eV)
0
5
10
∞
internuclear separation , R (Å)
He$^+$ + Hg
(1s) + (5d)^{10}(6s)^2
(1s)^2 + (5d)^{10}(7p)[$^2P^0_{3/2}$]
(1s)^2 + (5d)^9(6s)(6p)
(1s)^2 + (5d)^{10}(7p)[$^2P^0_{1/2}$]
He + Hg^{+*}

Figure 3

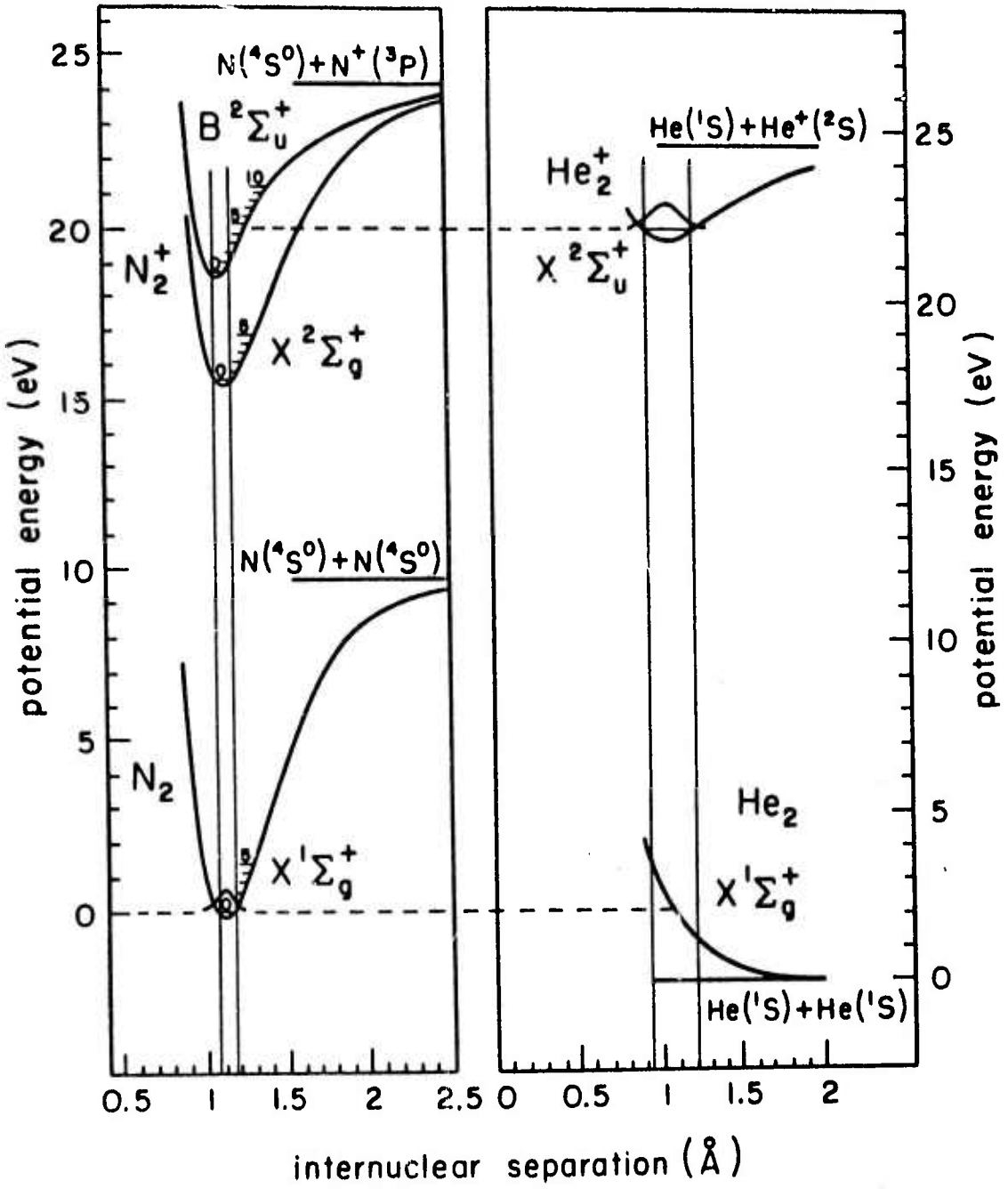
potential energy (eV)
25
20
15
10
5
0
N(⁴S⁰)+N⁺(³P)
B ²Σ⁺u
N₂⁺
X ²Σ⁺g
N(⁴S⁰)+N(⁴S⁰)
N₂
X ¹Σ⁺g
He(¹S)+He⁺(²S)
He₂⁺
X ²Σ⁺u
He₂
X ¹Σ⁺g
He(¹S)+He(¹S)
0.5
1
1.5
2
2.5
0
0.5
1
1.5
2
internuclear separation (Å)

Figure 4